Published in Physical Chemistry Chemical Physics 2010, vol 12, p 1131-1138
10.1039/b915486h

EXPERIMENTAL VERIFICATION OF THE METAL FLUX ENHANCEMENT IN A MIXTURE OF TWO METAL COMPLEXES: THE Cd/NTA/Glycine and Cd/NTA/Citric acid SYSTEMS

J. P. Pinheiro[a], J. Salvador[b], E. Companys[b], J. Galceran[b] and J. Puy[b*]

[a]*IBB/CBME, Department of Chemistry, Biochemistry and Pharmacy, Faculty of Sciences and Technology, University of Algarve, 8005-139 Faro, Portugal*

[b]*Departament de Química. Universitat de Lleida, Rovira Roure 191, 25198 Lleida, Spain*

* corresponding author jpuy@quimica.udl.es

ABSTRACT

Rigorous computation of the metal flux crossing a limiting surface of a system that contains a mixture of 1:1 metal complexes under steady-state planar diffusion in a finite domain and excess of ligand conditions predicts, for some cases, an enhancement of the metal flux with respect to that expected in a system with independent complexes. Indeed, the coupling of the dissociation kinetics of both complexes can yield higher metal fluxes than expected with important environmental implications. By using the voltammetric techniques AGNES and Stripping Chronopotentiometry, this paper provides experimental evidence of this enhancement for two systems: Cd/NTA/Glycine and Cd/NTA/Citric acid. The flux measured in both cases is in good agreement with the flux computed for the global system, exhibiting maximum enhancement ratios above 20%. Theoretical discussion of the flux enhancement factors and of the conditions for this enhancement are also provided.

Keywords: lability, metal complexation, flux enhancement, SCP, SSCP, AGNES

Published in Physical Chemistry Chemical Physics 2010, vol 12, p 1131-1138
10.1039/b915486h reprints also to galceran@quimica.udl.cat

1.- Introduction

The availability of metals to microorganisms or analytical sensors in natural systems is determined by a dynamic process that includes different steps, among which we find the internalization of the metal at the sensor/microorganism surface and the transport and interaction with ligands, particles and colloids present in the media [1].

Lability criteria predict which step is limiting the metal flux [2-8]: either the dissociation, in which case the system is called partially labile or inert, or the transport to the surface, in which case the system is called labile. Moreover, the lability degree has also been introduced to indicate the percentage of the complex contribution to the uptake flux with respect to its maximum contribution obtained when the kinetics of the complexation processes were fast enough to reach equilibrium at any time and relevant spatial position [3,4,7,9-11]. It has been shown that the lability degree depends on the kinetic constants, diffusion coefficients, size of the sensor, composition of the system, etc.

In a system with only one ligand, an increase of the ligand concentration decreases the lability degree of the complex due to the favouring of its association [3,12]. Despite mixtures of ligands correspond to the most common situation in natural media, only recently mixture effects have been described [13-17]. By rigorous simulation, it has been shown that the increase of the concentration of one ligand decreases the lability degree of its complex in the mixture as in the case of a single ligand system, but also influences the lability degree of the other complexes. Thus, interactions of the complexes in a mixture can play unexpected and relevant roles in the metal availability. For instance, it has been claimed that the addition of a small amount of a labile complex to a system with an almost inert one gives rise to an enhancement of the metal flux. Different systems fulfilling these conditions have been analyzed by simulation and the

enhancement has been justified by means of the reaction layer approximation which has been extended to mixtures of ligands [15-17]. However, no experimental evidence has been reported up to now of this flux enhancement.

Few analytical techniques for trace metal speciation analysis allow the determination of dynamic parameters. Of these, in recent years, we highlight the remarkable development of electroanalytical methods such as stripping chronopotentiometry, SCP [18], and scanned stripping chronopotentiometry, SSCP [19]. An additional and independent measurement of the free metal concentrations can be obtained from the voltammetric stripping technique AGNES [20].

It is the aim of this paper to provide experimental evidence of this enhancement by measuring the metal flux in different systems with a mercury electrode by using Scanned Stripping chronopotentiometry, SSCP. Two systems have been analyzed: Cd/NTA/Glycine and Cd/NTA/Citric acid, as two examples of a fixed inert complex (CdNTA) with two different labile complexes. Together with the discussion of the experimental results in section 4, the paper provides in section 2 an approximate analytical expression for the metal flux and for the enhancement factor, while section 3 gathers experimental information.

2.- Theoretical background

2.1 The system and its rigorous solution

For simplicity, let us restrict to consider a solution with a mixture of only 2 independent ligands $^{1}\mathrm{L}$ and $^{2}\mathrm{L}$ which can bind a metal ion M according to the scheme

$$\mathrm{M} + {}^{i}\mathrm{L} \underset{{}^{i}k_{\mathrm{d}}}{\overset{{}^{i}k_{\mathrm{a}}}{\rightleftharpoons}} \mathrm{M}\,{}^{i}\mathrm{L} \qquad i = 1, 2 \qquad (1)$$

where ${}^{i}K$, ${}^{i}k_{\mathrm{a}}$ and ${}^{i}k_{\mathrm{d}}$ are, respectively, the equilibrium and the association and dissociation kinetic constants of the complexation process to the ligand ${}^{i}\mathrm{L}$. Let us also assume that each ligand is present in the system in a great excess with respect to the metal, so that $c_{{}^{i}\mathrm{L}} \approx c^{*}_{{}^{i}\mathrm{L}}$ is constant at any spatial point. The corresponding equilibrium conditions read

$$ {}^{i}K' \equiv {}^{i}Kc^{*}_{{}^{i}\mathrm{L}} = \frac{{}^{i}k_{\mathrm{a}}c^{*}_{{}^{i}\mathrm{L}}}{{}^{i}k_{\mathrm{d}}} = \frac{{}^{i}k'_{\mathrm{a}}}{{}^{i}k_{\mathrm{d}}} = \frac{c^{*}_{\mathrm{M}{}^{i}\mathrm{L}}}{c^{*}_{\mathrm{M}}} \qquad (2) $$

In the deposition stage of SSCP, stirring actually limits the region of interest for reaction-diffusion to just the diffusion layer which can be approximately taken as a constant and is denoted as *g* in this work. Considering diffusion towards a planar surface in a finite diffusion domain of thickness *g*, the rigorous metal flux for steady state conditions can be written as [4].

$$ J_{\mathrm{M}} = D_{\mathrm{M}}\frac{c^{*}_{\mathrm{M}}}{g} + \sum_{i=1}^{2} D_{\mathrm{M}{}^{i}\mathrm{L}}\frac{c^{*}_{\mathrm{M}{}^{i}\mathrm{L}}}{g}{}^{i}\xi \qquad (3) $$

which indicates that the total metal flux can be understood as the addition of different contributions of the metal species (free metal and the different complexes) present in the system. The parameter ${}^{i}\xi$ is called the lability degree of the complex *i* and takes values in the range $0 < {}^{i}\xi < 1$, so that $D_{\mathrm{M}{}^{i}\mathrm{L}}\frac{c^{*}_{\mathrm{M}{}^{i}\mathrm{L}}}{g}$ is the maximum contribution of the complex $\mathrm{M}{}^{i}\mathrm{L}$. This maximum value reflects the transport limitation and is reached when there is no kinetic limitation in the dissociation of this complex.

${}^{i}\xi$ values can be obtained by solving a system of 3 linear diffusion equations corresponding to M, $\mathrm{M}{}^{1}\mathrm{L}$ and $\mathrm{M}{}^{2}\mathrm{L}$ as a particular case of the general methodology

95 developed for any number of ligands present [4,9,21,22]. These results will here be
96 referred to as "rigorous" simulation. When the complex does not contribute at all to the
97 metal flux ${}^{i}\xi = 0$, it is called inert and $J_{\mathrm{M}} = J_{\mathrm{free}} = D_{\mathrm{M}} \frac{c_{\mathrm{M}}^{*}}{g}$.

98

99 ## 2.2 The mixture effect in a system of two complexes

100 The analysis in ref. [4] of the behaviour of a system that contains one metal and a
101 mixture of ligands in steady state conditions showed that in general, the addition of an
102 inert ligand decreases the lability degree of all the complexes present in the system,
103 while the addition of a labile ligand tends to increase the lability degree of all of them.

104 Of practical relevance is the quantification of the mixture effect in the metal flux. In
105 order to measure this effect, let us define $J_{\mathrm{M}}^{n=1}$ as the flux resulting from the assumption
106 that the complexes keep the lability degree that they would have in simpler systems
107 with one complex at a time:

108 $$J_{\mathrm{M}}^{n=1} = D_{\mathrm{M}} \frac{c_{\mathrm{M}}^{*}}{g} + \sum_{i=1}^{2} D_{\mathrm{M}\,{}^{i}\mathrm{L}} \frac{c_{\mathrm{M}\,{}^{i}\mathrm{L}}^{*}}{g}\, {}^{i}\xi^{n=1} \qquad (4)$$

109 where ${}^{i}\xi^{n=1}$ is the lability degree of complex *i* in a single ligand system. Notice that Eqn
110 (4) is formally identical to Eqn. (3) with the only change of ${}^{i}\xi$ by ${}^{i}\xi^{n=1}$. $J_{\mathrm{M}}^{n=1}$
111 corresponds, then, to the value expected in a mixture of independent complexes, i. e.,
112 without interactions effects between the respective lability degrees. As previously
113 reported [3], ${}^{i}\xi^{n=1}$ can be rigorously computed as:

114 $${}^{i}\xi^{n=1} = \frac{{}^{i}\zeta - \tanh {}^{i}\zeta}{{}^{i}\zeta + {}^{i}\varepsilon\ {}^{i}K \tanh {}^{i}\zeta} \qquad (5)$$

115 where

$$ {}^{i}\zeta = g\sqrt{\frac{{}^{i}k_{\mathrm{d}}\left(1+{}^{i}\varepsilon\ {}^{i}K^{'}\right)}{{}^{i}\varepsilon\ D_{\mathrm{M}}}} \qquad (6) $$

The evaluation of Eqn. (3) and Eqn. (4) is performed using common values of the parameters, in particular, a ligand concentration equal to that of the mixture.

The parameter ${}^{i}\zeta$ in Eqn (6) can be thought of as (approximately) a normalized dimensionless inverse reaction layer, given that for the usual case of interest $({}^{i}\varepsilon\ {}^{i}K^{'} >> 1)$

$$ {}^{i}\zeta \approx g\sqrt{\frac{{}^{i}k_{\mathrm{a}}^{'}}{D_{\mathrm{M}}}} = \frac{g}{{}^{i}\mu} \qquad (7) $$

A good approximation to Eqn. (4) is $({}^{i}\varepsilon\ {}^{i}K' >> 1, \quad g >> {}^{i}\mu)$

$$ {}^{i}\xi^{n=1} \approx \frac{g}{g+{}^{i}\varepsilon\ {}^{i}K'\sqrt{D_{\mathrm{M}}/\ {}^{i}k_{\mathrm{a}}'}} \qquad (8) $$

A system with only two complexes can be understood as the addition of the more labile to the more inert or just in the reverse order. Their mutual influence on the lability degree is opposite, so that the global effect at the level of the resulting metal flux is - due to partial cancellation - less pronounced than expected from the changes in the particular lability degrees. However, there are situations in which there is a non-negligible net result. Under these conditions, important deviations of the metal flux from the value expected from the lability degrees of the single ligand system can arise. For instance, if a ligand forming a labile complex is added to a system that contains an almost inert complex, even a small proportion of the labile complex can lead to an enhancement of the metal flux over the value expected from independent complexes. As we will see, under these conditions, we have an increase of the lability of the inert complex (by the interaction with the labile one) that increases the metal flux, while the

effect of the inert one on the labile complex is negligible on the metal flux due to: i) the low concentration of the labile complex and ii) to the fully labile character of this complex which prevents its shifting towards a lower lability degree.

Quantitatively, the metal flux enhancement factor can be defined as [16,17]:

$$\sigma = \frac{J_{\mathrm{M}}}{J_{\mathrm{M}}^{n=1}} \tag{9}$$

2.3 Analytical expressions for the enhancement factor.

Rigorous expression for the limiting case of one fully labile complex in the mixture

A simple analytical expression for the metal flux can be obtained from the rigorous solution given in the supplementary information of [4] by considering the limiting case where one complex, for instance $\mathrm{M}^{2}\mathrm{L}$, is fully labile ($^{2}k_{\mathrm{d}} \to \infty$) while the other is not:

$$J_{\mathrm{M}} = \frac{D_{\mathrm{M}} c_{\mathrm{M}}^{*}}{g} \frac{\left(1 + {}^{1}\varepsilon\ {}^{1}K' + {}^{2}\varepsilon\ {}^{2}K'\right)}{1 + \dfrac{{}^{1}\varepsilon\ {}^{1}K'}{\left(1 + {}^{2}\varepsilon\ {}^{2}K'\right)} \dfrac{\tanh\zeta}{\zeta}} \tag{10}$$

with

$$\zeta = g\sqrt{\frac{{}^{1}k_{\mathrm{d}}\left(1 + {}^{1}\varepsilon\ {}^{1}K' + {}^{2}\varepsilon\ {}^{2}K'\right)}{D_{\mathrm{M}}\ {}^{1}\varepsilon\left(1 + {}^{2}\varepsilon\ {}^{2}K'\right)}} \tag{11}$$

The corresponding lability parameters in the mixture are

$$^{1}\xi = \frac{1 - \dfrac{\tanh\zeta}{\zeta}}{1 + \dfrac{{}^{1}\varepsilon\ {}^{1}K'}{\left(1 + {}^{2}\varepsilon\ {}^{2}K'\right)} \dfrac{\tanh\zeta}{\zeta}} \quad ; \quad {}^{2}\xi = 1 \tag{12}$$

Eqn. (10) leads to a very simple expression for the enhancement factor defined in (9)

$$\sigma = \frac{\left(1+ {}^1\varepsilon\ {}^1K' + {}^2\varepsilon\ {}^2K'\right)}{\left(1+\frac{{}^1\varepsilon\ {}^1K'}{\left(1+ {}^2\varepsilon\ {}^2K'\right)}\frac{\tanh\zeta}{\zeta}\right)\left(1+ {}^1\varepsilon\ {}^1K'\frac{{}^1\zeta - \tanh {}^1\zeta}{{}^1\zeta + {}^1\varepsilon\ {}^1K \tanh {}^1\zeta} + {}^2\varepsilon\ {}^2K'\right)} \quad (13)$$

Conditions for the maximum enhancement

In order to have a rough estimate of the conditions for which the enhancement is produced, we observe that the plot of the enhancement factor (Fig 1) as given by eqn. (13) exhibits a maximum. The position of this maximum will essentially correspond to the minimum of the denominator in (13). Taking ${}^1\varepsilon={}^2\varepsilon=1$, $\tanh\ \zeta =1$, $\tanh\ {}^1\zeta =1$, $1<<{}^2K'<<{}^1K'$, ${}^1K' >> {}^2K'\zeta$ and ${}^1\zeta <<{}^1K'$, the denominator can be written as

$$\sqrt{\frac{{}^1K' D_M}{g^2\ k_d\ {}^2Kc_{{}^2L}}}\left({}^1\zeta + {}^2Kc_{{}^2L}\right) \quad (14)$$

The condition we seek is:

$$\frac{d}{dc_{{}^2L}}\left(\frac{{}^1\zeta}{\sqrt{c_{{}^2L}}} + {}^2K\sqrt{c_{{}^2L}}\right) = 0 \quad (15)$$

so that the extreme condition can be written as

$${}^2Kc_{{}^2L} = {}^1\zeta \approx \frac{g}{{}^1\mu} \quad (16)$$

Expression (16) gives the concentration of the labile ligand, here labelled as ${}^2L$, to be added into a solution of the metal and the almost inert ligand, here labelled as ${}^1L$, to obtain the maximum enhancement effect.

With respect to $c_{{}^1L}$ (the concentration of the inert ligand), expression (13) indicates that σ increases monotonically with increasing $c_{{}^1L}$. Although σ could be huge for very large $c_{{}^1L}$, the absolute value of the metal flux could be negligible.

In order to look for a physical interpretation of the condition for the maximum, we re-write eqn. (16) as

$$D_{M^2L}\frac{c^*_{M^2L}}{g} \approx D_M \frac{c^*_M}{{}^1\mu} \qquad (17)$$

We have multiplied both terms by the equal diffusion coefficients (${}^1\varepsilon=1$) in order to obtain on the l.h.s. the flux of the labile complex and on the r.h.s. the flux of the inert complex. In this way, the maximum condition would stem from a similar contribution to the flux of the fully labile and inert complexes.

In practice, expression (16) could be useful as a quick guideline of the conditions suitable for the enhancement effect to be noticeable.

3. Experimental

3.1. Reagents

All solutions were prepared in ultrapure water from MilliQ Simplicity (resistivity > 18 MΩ cm). Cd(II) stock solutions were prepared from dilution of cadmium standard solutions (1000 mg/L Merck), and the $NaNO_3$ used to adjust the ionic strength solution was prepared from the solid (Merck, suprapur). Stock solution MOPS (3-(N-morpholino)propanesulfonic acid) buffer was prepared from the solid (Sigma-Aldrich, SigmaUltra >99.5%). HNO_3 (Merck, suprapur) and KOH (solid from Fluka, p.a.) solutions were used to adjust the pH.

Nitrilotriacetic acid (NTA), Glycine and Citric acid were prepared from the solid (Fluka, puriss p.a.).

3.2. Electrochemical experiments

SCP/SSCP and AGNES experiments were performed in the same day using an Eco Chemie Autolab PGSTAT12 potentiostat in conjunction with a Metrohm 663VA stand and a personal computer using the GPES 4.9 software (Eco Chemie). Electrodes included a static mercury drop electrode (radius 1.78×10^{-4} m for the SCP/SSCP experiments and 1.41×10^{-4} m for the AGNES experiments, Fluka mercury p.a.) (working electrode), a saturated calomel electrode with a 0.10 M $NaNO_3$ salt bridge (reference electrode), and a glassy carbon counter electrode. Measurements were performed at 25.0^{o}C in a reaction vessel thermostated with a bath (Selecta, Unitronic 100). A glass combined electrode (Orion 9103) was attached to a Thermo Orion 720Aplus ion analyzer to control the pH.

SSCP/AGNES calibration:

SCP/SSCP and AGNES experiments (which were performed in the same electrochemical cell) require a calibration plot at the same ionic strength (0.10M) as the main measurement. For AGNES, a three point calibration was performed (usually at 1.6, 3.2 and 5.0×10^{-4} mol m^{-3} of total metal concentration) after which the SSCP calibration was done at the highest concentration. The calibrations were performed at low pH (< 4) in order to avoid losses to the container walls.

SSCP and AGNES combined experiments:

When both SSCP and AGNES techniques were used in the same solution, after the calibrations, NTA (2×10^{-3} mol m^{-3}) was added directly to the calibration solution, together with MOPS pH buffer. The pH was adjusted to 8.00±0.05 and SSCP and AGNES data were acquired.

SCP/SSCP titrations:

The process was parallel to the previous case, but only the SSCP calibration was performed. Then, the labile ligand was added in the range 5×10^{-2} to 4 mol m^{-3} for Citric acid and from 1×10^{-1} to 10 mol m^{-3} for Glycine and the SCP data were acquired for each addition.

3.2.1. SCP/SSCP parameters

Stripping chronopotentiometry techniques have two steps: deposition and quantification. During the deposition step (accumulation) the metal ions are reduced at a constant potential (-0.75V for Cd(II) *vs.* SCE) well above the standard reduction potential of the metal for a given time interval, the deposition time, t_d (60 s in this work).

The quantification of the metal ion accumulation is performed during the so-called stripping step when the metal ion is oxidized by application of a constant oxidizing current, I_s, of 1×10^{-9}A in quiescent solution until the potential reached a value sufficiently beyond the transition plateau (-0.40 V for Cd(II)). The I_s value corresponds to conditions that approach complete depletion (the product $I_s\tau$ is constant, for decreasing I_s values). The experimental signal is called the limiting transition time (τ^*) calculated from the integral of the dt/dE *vs.* E curve obtained from the raw data (potential vs. time [18]).

In the case of SSCP, a series of measurements is made over a range of deposition potentials, E_d. The transition time values are then represented against the deposition

potential, τ *vs.* E_d. The resulting plots, called SSCP curves, are formally equivalent to a voltammogram. The limiting transition time (τ^*, equivalent to the SCP result) and the half-wave potential ($E_{1/2}$) are the most useful experimental parameters extracted from these curves.

3.2.2. AGNES parameters

A DPP experiment with the largest mercury drop (radius 2.03×10^{-4} m) was performed during the calibration, so that, from its peak potential, we could compute the *E*-value corresponding to the desired preconcentration factor or gain *Y* for any of the steps of the AGNES experiment [20]. The potential program for the AGNES experiment consisted in applying three potential steps [23]:

i) $E_{1,a}$ under reduction diffusion limited conditions, corresponding to $Y_{1,a} = 1\times10^{8}$ for a time $t_{1,a}$ (with stirring). The suitable $t_{1,a}$ depends on the desired gain Y (or $Y_{1,b}$) applied: from previous experiments, it is known that $t_{1,a}$ = 35 s for $Y_{1,b}$ = 50;

ii) $E_{1,b}$ corresponding to the desired $Y_{1,b}$ for a $t_{1,b}$ longer always than $3t_{1,a}$, (with stirring) and waiting time t_w = 50 s (without stirring). The value of $Y_{1,b}$ was selected to yield a current above the limit of detection;

iii) E_2 corresponding to $Y_2 = 1\times10^{-8}$ under re-oxidation diffusion limited conditions for 50 s, with the response current being read at t_2 = 0.20 s.

To subtract other components of the measured current different than the faradaic one, the shifted blank (see [24]) was performed with Y_1 = 0.01 (a negligible *Y* compared to the $Y_{1,b}$ of the main measurement).

4.- Results and discussion

4.1. Retrieving information from SSCP/SCP

A) Stability constant

For the depletion mode of scanned stripping chronopotentiometry (SSCP) [19] a known rigorous equation is available for the full wave in the kinetic current regime [25]. With this expression, the characteristic parameters of the SSCP wave (τ^* and $E_{d,1/2}$) can be used to obtain information on the lability of metal complex systems [26].

The thermodynamic complex stability constant, *K*, can be calculated from the shift in the half-wave deposition potential, $\Delta E_{d,1/2}$, (analogous to the DeFord-Hume expression) irrespective of the degree of lability of the system [26]:

$$\ln(1+K') = -(nF/RT)\Delta E_{d,1/2} - \ln\left(\tau^*_{M+L}/\tau^*_{M}\right) \quad (18)$$

where τ^*_{M+L} and τ^*_{M} denote the τ values for limiting deposition current conditions in the presence and in the absence of ligand, respectively. The values obtained for Cd-NTA, Cd-Citrate and Cd-Glycine are reported in Table 1. The corresponding bulk free Cd concentration values were confirmed with AGNES experiments.

B) Kinetic constants

The limiting transition time is proportional to the deposited charge. In a system of one complex ML, the limiting deposition flux can be expressed in terms of the lability degree of this complex (see eqn (4)) as:

$$I_S\tau^*_{ML} = I^*_d t_d = nFA\frac{D_M c^*_M}{g}(1+\varepsilon K'\xi)t_d \quad (19)$$

where I^*_d is the limiting deposition current and *A* is the area of the electrode. Once the value of ξ is found from eqn (19), the value of k_a' can be computed from eqn (4) or its

approximation, Eqn. (8) ($^{i}\varepsilon\ ^{i}K' >> 1, \quad g >> {}^{i}\mu$). Alternatively, one can proceed by simply dividing (19) by its only metal limiting expression:

$$\frac{\tau^{*}_{M+L}}{\tau^{*}_{M}} = 1 + \varepsilon K' \xi \qquad (20)$$

From SSCP data in a solution with $c_{T,NTA}$ = 2×10^{-3} mol m^{-3} and $c_{T,Cd}$ = 5×10^{-4} mol m^{-3}, via expression (20), we obtained ξ, from which the effective or conditional association constant (k_a') for Cd-NTA was computed with equation (8) (see Table 1). Other kinetic constants follow from Eigen expression and are also reported in Table 1.

Note that recently, van Leeuwen *et al.* [25] analysed quantitatively the impact of ligand protonation on metal speciation dynamics, showing that the metal complexation process to the different protonated species of the ligand can be reduced to only one complexation process with an effective association constant which depends on the intrinsic association constants of the various protonated forms and on the pH. Thus, results reported in Table 1 for the kinetic constants have to be considered as effective or conditional values for the ionic strength and pH considered in this work.

4.2 Experimental fluxes in mixtures

A) Cd/NTA/Citric acid system

A replicate SSCP experiment with $c_{T,NTA}$ = 2×10^{-3} mol m^{-3} and $c_{T,Cd}$ = 5×10^{-4} mol m^{-3} has been conducted by adding Citric acid to the system in the concentration range $c_{T,Cit}$ = 5×10^{-2} mol m^{-3} up to $c_{T,Cit}$ = 1.6 mol m^{-3}. As the Citric concentration increases the metal flux in the deposition step also increases up to a factor 3 as it is shown in Fig. 2 (see markers (×) and (+)). It could be thought that this increase is due to the shift of the bulk equilibrium towards the formation of Cd-Citrate, a labile complex. However, a

simple speciation calculation predicts that although the free Citrate concentration reached is higher than the NTA^{3-} concentration by 4 orders of magnitude, the species Cd-NTA is still the dominant complex (i.e. most abundant) since ${}^{NTA}K' >> {}^{Cit}K'$.

Fig. 2 also shows a quite good reproducibility of the two replicate experiments and the agreement of these results with the theoretical ones obtained for the mixture system, either by rigorous numerical solution (continuous line), by assuming the Citrate as fully labile and using Eqn. (10) (dotted line) or by using the reaction layer approximation [15,16] which is here implemented by using equation 15 given in ref [16], (see dotted-dashed line). However, the theoretical results without considering the interaction between both complexes, i.e., calculated with Eqn. (4) and shown in Fig. 2 in dashed line, clearly diverge from the experimental ones underestimating the flux. The difference between this dashed line and the experimental measurements corresponds to the enhancement term, so that the existence of the metal flux enhancement due to the mixture effect is clearly evidenced in the figure.

The availability of the rigorous simulation tools allows for a detailed analysis of the enhancement conditions in the present system. The mutual influence of both complexes in the respective lability degrees is depicted in Fig. 3. As can be seen, the Cd-Citrate complex is almost fully labile and the mixture does not modify noticeably the lability degree of this complex. Additionally, the Cd-NTA complex appears as almost inert with a lability degree slightly increasing as the concentration of the Citric acid in the system increases. The influence of the changes of concentrations and lability degrees on the metal flux can be analyzed in Fig. 4. The contribution of the Cd-Citrate complex to the global flux (see full squares), given by

$$J_{\text{Cd-Cit}} = D_{\text{Cd-Cit}} \frac{c^{*}_{\text{Cd-Cit}}}{g}\ {}^{\text{Cd-Cit}}\xi \qquad (21)$$

increases almost linearly as the total concentration of Citrate increases. However, $J_{\text{Cd-Cit}}$ does not show any difference from the Cd-Citrate contribution expected in a system where the interaction between both complexes was frozen

$$J^{\text{n=1}}_{\text{Cd-Cit}} = D_{\text{Cd-Cit}} \frac{c^{*}_{\text{Cd-Cit}}}{g}\ {}^{\text{Cd-Cit}}\xi^{n=1} \qquad (22)$$

This behaviour is consistent with this complex being fully labile, both in the single ligand system and in the mixture (see Fig. 3), so that its contribution is not influenced by the presence of the NTA in the system.

The contribution of the Cd-NTA complexes to the metal flux is the most important one for $c_{\text{T,Cit}} < 1.7\,\text{mol}\times\text{m}^{-3}$ (see triangles in Fig. 4), and the impact of this influence in the mixture (in comparison with the single ligand system) is just the responsible for the difference between J_{M} and $J^{n=1}_{\text{M}}$. Thus, the increase of the lability degree of the almost inert complex, due to the addition into the system of the labile Citric acid, albeit low, is the responsible of the enhancement of the metal flux. The enhancement factor σ as defined in (13) reaches 1.2

The concentration profiles can help in understanding the physical basis of the enhancement effect. Fig. 5 shows the concentration profiles of the metal and the Cd-NTA complexes at 3 points of the titration corresponding to concentrations of added Citric acid of 1, 2 and 8×10^{-1} mol m^{-3}, respectively. The profile of the metal-Citrate complex converges with the normalized metal profile beyond its small particular

reaction layer and it is not depicted in the figure. Only the profile of the Cd-NTA complex is depicted, as this complex is the responsible of the metal enhancement flux.

This figure deserves some comments: i) the metal concentration profile is depleted as Citrate is added into the system. This decrease in the Cd-profile favours the dissociation of Cd-NTA complex in all the diffusion domain, increasing its contribution to the metal flux as shown in Fig. 4 and being the way by which the flux enhancement is produced (i.e. the metal concentration profile can be seen as the coupling mechanism).

ii) Numerical simulation in the literature shows that, due to the addition of the labile ligand into the system, the reaction layer of the inert one increases [4,16]. As beyond the reaction layer the complex is in equilibrium with the metal, the net dissociation takes place within the reaction layer, so that the increase of the thickness of this layer (due to the addition of the labile ligand) justifies the flux enhancement effect. No increase of the reaction layer thickness of the Cd-NTA is seen in Fig. 5 along the addition of Citric acid into the system. Thus, a noticeable mixture effect can arise even when the change in the reaction layer is hardly detectable as in the present case. Notice that, in the present case, the reaction layer of Cd-NTA cannot increase since it extents over all the diffusion domain in Fig. 5.

iii) The metal flux is (for finite dissociation rates of the involved complexes) proportional to the gradient of the free metal concentration at the electrode surface, so that the gradient of the metal profile should be larger as the Citrate concentration increases (see Fig. 5). As this is hardly seen in the main picture of fig. 5, a magnification of the profiles close to the electrode surface up to distances of the order of the composite reaction layer of the Cd-Citrate complex is included as inset of Fig. 5.

This magnification allows to clearly see a crossing of the metal concentration profiles, so that the lowest metal concentration profile in the main figure (corresponding to a Citrate concentration of 0.8 mol m^{-3}) decreases slowly until it steeply falls to the zero value within a close approach of the electrode, so that it yields the highest metal gradient at the electrode surface.

The application of condition (16) with the parameters of the Citrate titration predicts a maximum (see Fig 1) at $c_{^2\mathrm{L}} = c_{\mathrm{Cit}} \approx 1.124$ mol m^{-3} which is a rough approximation to the real position of the maximum $c_{^2\mathrm{L}} = c_{\mathrm{Cit}} \approx 0.847$ mol m^{-3}. The corresponding σ -values (computed with Eqn. (13)) are 1.313 (for the true maximum) and 1.279 (using the approximate $c_{^2\mathrm{L}}$ from Eqn. (16)).

B) The Cd/NTA/Glycine system

In two experiments that cover different Glycine concentration ranges, Glycine has been added into a system with $c_{\mathrm{T,Cd}} = 5\times10^{-4}$ mol m^{-3} and $c_{\mathrm{T,NTA}} = 2\times10^{-3}$ mol m^{-3} in the range $c_{\mathrm{T,Gly}} = 0.1 \ldots 9.3$ mol m^{-3}. Increasing the Glycine concentration, the metal flux increases (Fig. 6). The main result of this figure is that there is also a good convergence of the theoretical results of the mixture system (at the rigorous level, by using Eqn (10) or by using the reaction layer approximation, Eqn. 15 in ref. [16]) with the experimental ones, while the theoretical results given by Eqn. (4) that neglect the interaction between the complexes diverge yielding lower flux values. An enhancement of the metal flux is then evidenced in the figure. As the conditional stability constant ${}^{\mathrm{CdNTA}}K'$ is higher than ${}^{\mathrm{CdGly}}K'$, Cd ions are preferentially bound to NTA even at the highest Glycine concentration, being the concentration of Cd bound to Glycine rather negligible.

Fig. 7 depicts the change of the lability degrees. Notice that now, a decrease of the lability of the more labile complex is seen in the figure due to the presence of NTA in the system, while the lability degree of Cd-NTA increases due to the addition of Glycine into the system.

However, the difference between J_{CdGly} and $J^{n=1}_{\mathrm{CdGly}}$ is negligible, see Fig. 8, and again, the enhancement of the metal flux is due to the enhancement of $J_{\mathrm{Cd\,NTA}}$ in the interacting mixture.

The concentration profiles of the free Cd and the Cd-NTA complex are similar to those reported in Fig. 5 and are not included here.

With the parameters of the Glycine titration (used in Fig 6), the maximum enhancement factor appears at $c_{^2\mathrm{L}} = c_{\mathrm{Gly}} \approx 0.137$ mol m^{-3} (where σ= 1.312) while the approximation (16) yields $c_{^2\mathrm{L}} = c_{\mathrm{Gly}} \approx 0.182$ mol m^{-3} (with a σ= 1.306 computed with eqn. (13)), which means a good approximation for the σ -value.

Conclusion

The lability degree of a complex is not an intrinsic property of this complex, but a property influenced by the concentration of the rest of complexes of this metal that exist in the solution. As a consequence of this influence, an enhancement of the limiting metal flux crossing a consuming surface was predicted by numerical simulation when a labile ligand is added into a system with an almost inert complex.

This prediction is here experimentally measured for the Cd/NTA/Glycine and Cd/NTA/Citric acid systems. Cd-NTA complexes behave as almost inert complexes in

SCP experiments under the concentrations reported in the present work. Cd-Glycine and Cd-Citric behave as labile complexes under the same conditions. The enhancement factor reaches 20% of the metal flux for the case of the Cd-NTA-Citrate mixture.

A detailed analysis has shown that, for both cases, the enhancement is due to the increase of the lability of the Cd-NTA complexes when Glycine or Citric acid is added. As a general mechanism, this increase in the lability degree can be related to the depletion of the metal concentration profile when the labile ligand is added into the system.

Simple approximate analytical expressions for the enhancement factor have been reported. These expressions have been used to obtain an estimation of the concentration of the labile ligand to be added to obtain the highest enhancement factor. These estimations are in agreement with the experimental measurements.

Acknowledgments

J.P.P. acknowledges the funding received by “IBB/CBME, LA, FEDER/POCI 2010” and a sabbatical grant SFRH/BSAB/855/2008 from Fundação para a Ciência e Tecnologia, Portugal. This work was also financially supported by the Spanish Ministry of Education and Science (Projects CTQ2006-14385 and CTM2006-13583) and from the “Comissionat per a Universitats i Recerca del Departament d’Innovació, Universitats i Empresa de la Generalitat de Catalunya”

References

[1] J.Buffle, Complexation Reactions in Aquatic Systems. An Analytical Approach., Ellis Horwood Limited, Chichester, 1988.

[2] H.P.van Leeuwen, Electroanal. 13 (2001) 826.

[3] J.Salvador, J.Puy, J.Cecilia, J.Galceran, J. Electroanal. Chem. 588 (2006) 303.

[4] J.Salvador, J.Puy, J.Galceran, J.Cecilia, R.M.Town, H.P.van Leeuwen, J. Phys. Chem. B 110 (2006) 891.

[5] R.A.G.Jansen, H.P.van Leeuwen, R.F.M.J.Cleven, M.A.G.T.van den Hoop, Environ. Sci. Technol. 32 (1998) 3882.

[6] H.P.van Leeuwen, Environ. Sci. Technol. 33 (1999) 3743.

[7] J.Galceran, J.Puy, J.Salvador, J.Cecília, H.P.van Leeuwen, J. Electroanal. Chem. 505 (2001) 85.

[8] W.Davison, J. Electroanal. Chem. 87 (1978) 395.

[9] J.Galceran, J.Puy, J.Salvador, J.Cecília, F.Mas, J.L.Garcés, Phys. Chem. Chem. Phys. 5 (2003) 5091.

[10] J.Galceran, H.P.van Leeuwen, in H. P. van Leeuwen and W. Koester (Eds.), Physicochemical kinetics and transport at chemical-biological surfaces. IUPAC Series on Analytical and Physical Chemistry of Environmental Systems, John Wiley, Chichester (UK), 2004, Chapter 4, p. 147.

[11] J.P.Pinheiro, J.Galceran, H.P.van Leeuwen, Environ. Sci. Technol. 38 (2004) 2397.

[12] J.P.Pinheiro, R.F.Domingos, M.Minor, H.P.van Leeuwen, J. Electroanal. Chem. 596 (2006) 57.

[13] J.Salvador, J.L.Garcés, J.Galceran, J.Puy, J. Phys. Chem. B 110 (2006) 13661.

[14] J.Salvador, J.L.Garcés, E.Companys, J.Cecilia, J.Galceran, J.Puy, R.M.Town, J. Phys. Chem. A 111 (2007) 4304.

[15] Z.S.Zhang, J.Buffle, J. Phys. Chem. A 113 (2009) 6562.

[16] Z.S.Zhang, J.Buffle, R.M.Town, J.Puy, H.P.van Leeuwen, J. Phys. Chem. A 113 (2009) 6572.

[17] Z.S.Zhang, J.Buffle, Environ. Sci. Technol. DOI: 10.1021/es9003526 (2009)

[18] R.M.Town, H.P.van Leeuwen, J. Electroanal. Chem. 509 (2001) 58.

[19] H.P.van Leeuwen, R.M.Town, Environ. Sci. Technol. 37 (2003) 3945.

[20] J.Galceran, E.Companys, J.Puy, J.Cecília, J.L.Garcés, J. Electroanal. Chem. 566 (2004) 95.

[21] D.R.Turner, M.Whitfield, J. Electroanal. Chem. 103 (1979) 43.

[22] D.R.Turner, M.Whitfield, J. Electroanal. Chem. 103 (1979) 61.

[23] E.Companys, J.Cecília, G.Codina, J.Puy, J.Galceran, J. Electroanal. Chem. 576 (2005) 21.

503 [24] J.Galceran, C.Huidobro, E.Companys, G.Alberti, Talanta 71 (2007) 1795.

504 [25] H.P.van Leeuwen, R.M.Town, J. Electroanal. Chem. 561 (2004) 67.

505 [26] J.P.Pinheiro, H.P.van Leeuwen, J. Electroanal. Chem. 570 (2004) 69.

506
507

Published in Physical Chemistry Chemical Physics 2010, vol 12, p 1131-1138
10.1039/b915486h
reprints also to galceran@quimica.udl.cat

508 TABLE

509 Table 1: Parameters used in the theoretical calculation of the fluxes and bulk
510 concentrations. pH = 8; $g = 2.2\times10^{-5}$ m; $\varepsilon_1 = \varepsilon_2 = 1$.

Protonation constants			
	NTA	**Citrate**	**Glycine**
log ($K_{H,1}$ /m^3 mol^{-1})	6.73	2.7	6.6
log ($K_{H,2}$ /m^3 mol^{-1})	-0.5	1.35	-0.63
log ($K_{H,3}$ /m^3 mol^{-1})	-1.1	-0.09	-
Complexation constants			
log ($K_{Cd\text{-}L}$ /m^3 mol^{-1})	6.80	0.71	1.50
log ($k_{a\ (Cd\text{-}L)}$ /m^3 mol^{-1})	6.26	7.42	5.79

511

512 FIGURES

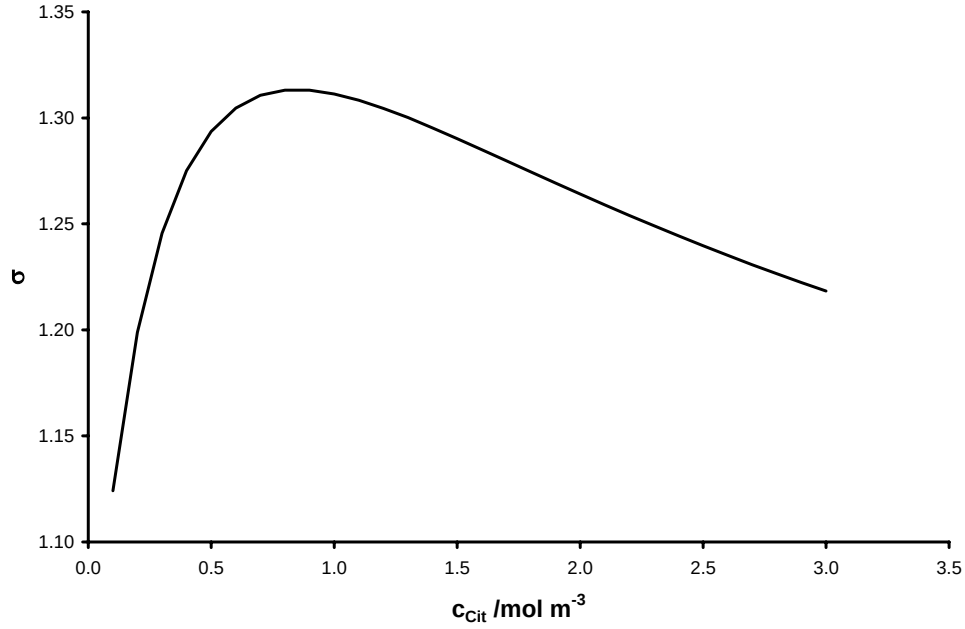

513

514 Fig 1: Enhancement factor (σ) computed with eqn. (13) for the Cd+NTA+Citric system

515 with parameters in Table 1 and c_{NTA} = 2.79×10^{-5} mol m^{-3}, showing a maximum at

516 c_{Cit} ≈0.85 mol m^{-3}.

517

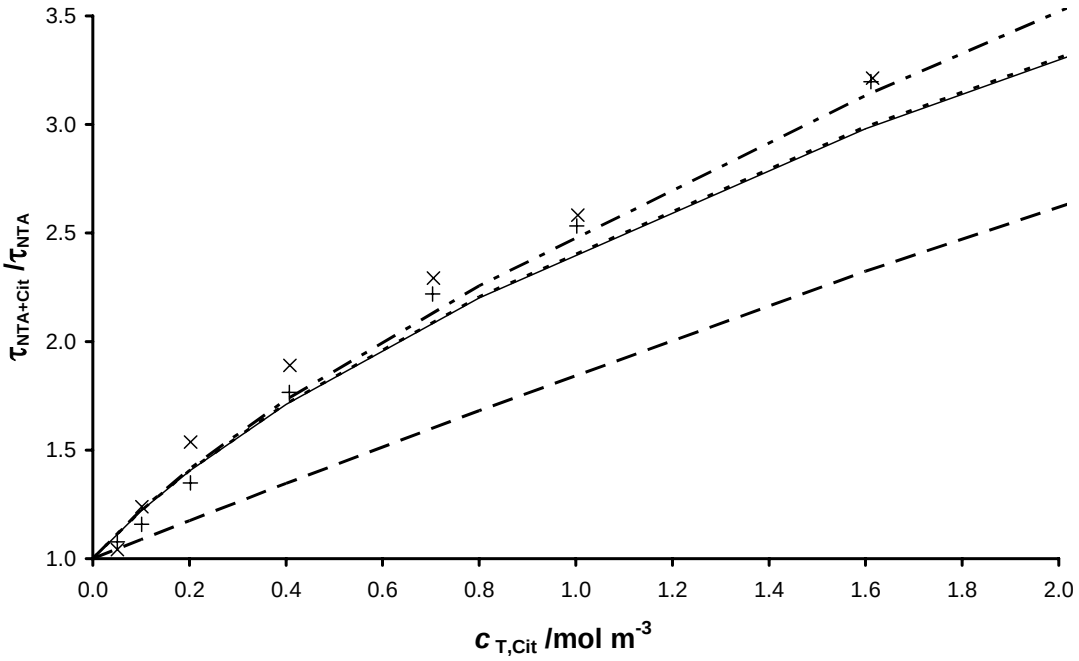

518

519 Fig 2: Ratio of fluxes after and before the addition of different amounts of Citrate to a
520 system initially containing $c_{T,NTA} = 2\times10^{-3}$ mol m^{-3} and $c_{T,Cd} = 5\times10^{-4}$ mol m^{-3}. Markers
521 (×) and (+) stand for two replicate series and continuous line for the rigorous solution
522 with parameters in Table 1. Dotted line corresponds to the limiting case of full lability
523 of CdCit (Eqn (10)) and dashed line stands for the case of non-interacting complexes
524 (Eqn 4). Dotted-dashed line corresponds to the Zhang and Buffle approximation [15-
525 16].
526

527

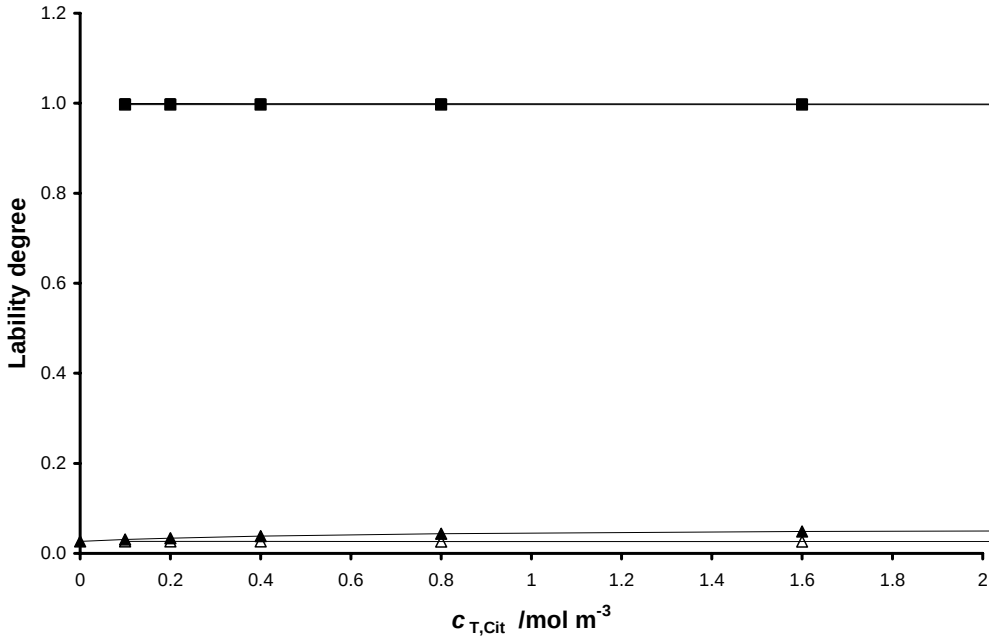

528

529 Fig 3: Lability degrees of complexes Cd+NTA+Citrate along the titration corresponding
530 to Fig 2 with parameters in Table 1. Markers: Full triangle for ${}^{\mathrm{CdNTA}}\xi$; open triangle for
531 the hypothetical case with no interaction ${}^{\mathrm{CdNTA}}\xi^{n=1}$; full square for ${}^{\mathrm{CdCit}}\xi$; open square
532 for the hypothetical case with no interaction ${}^{\mathrm{CdCit}}\xi^{n=1}$. In the figure, ${}^{\mathrm{CdCit}}\xi \approx {}^{\mathrm{CdCit}}\xi^{n=1}$ so
533 that open squares coincide with full squares.

Published in Physical Chemistry Chemical Physics 2010, vol 12, p 1131-1138
10.1039/b915486h
reprints also to galceran@quimica.udl.cat

534

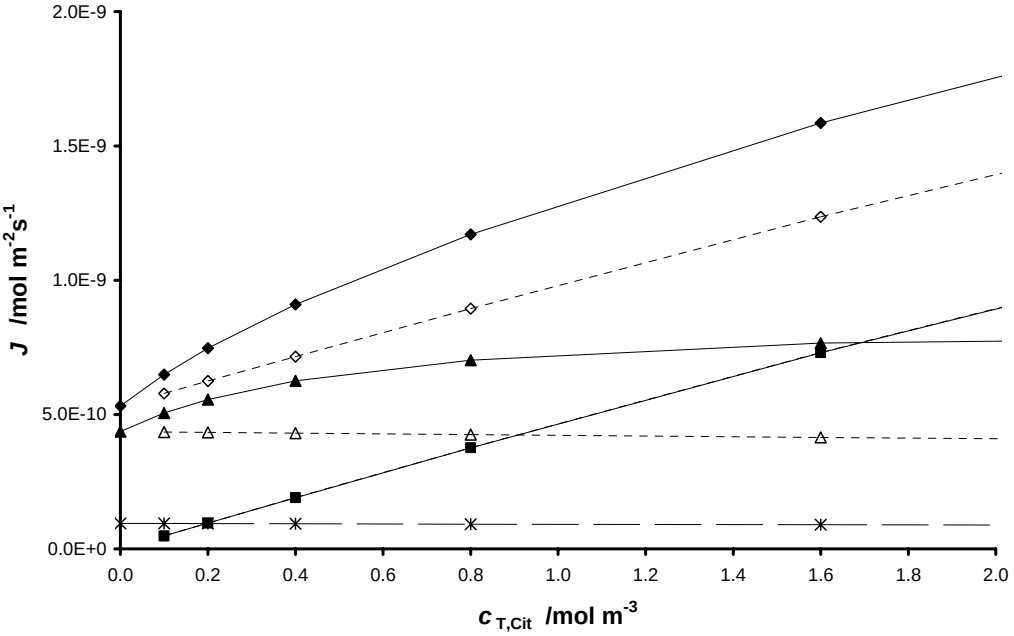

535

536 Fig 4: Fluxes and their components along the titration corresponding to Fig 2 with
537 parameters in Table 1. Solid line stands for the rigorous solution, dotted line stands for
538 fluxes without interaction and dashed line for the free metal contribution. Markers: full
539 diamond for the rigorous total flux, J_M; open diamond for the hypothetical total flux
540 when there is no interaction between complexes $J_M^{n=1}$ (eq 4); asterisk for free metal
541 component, $J_{free} = D_M c_M^* / g$; full triangle for the flux associated to the complex CdNTA,
542 $J_{CdNTA} = D_{CdNTA} c_{CdNTA}^{*\,CdNTA} \xi / g$; full square for the flux $J_{CdCit} = D_{CdCit} c_{CdCit}^{*\,CdCit} \xi / g$; open
543 triangle for the hypothetical flux with no interaction $J_{CdNTA}^{n=1} = D_{CdNTA} c_{CdNTA}^{*\,CdNTA} \xi^{n=1} / g$;
544 and open square (coinciding with the full squares in this figure) for the hypothetical flux
545 with no interaction $J_{CdCit}^{n=1} = D_{CdCit} c_{CdCit}^{*\,CdCit} \xi^{n=1} / g$.

546

547

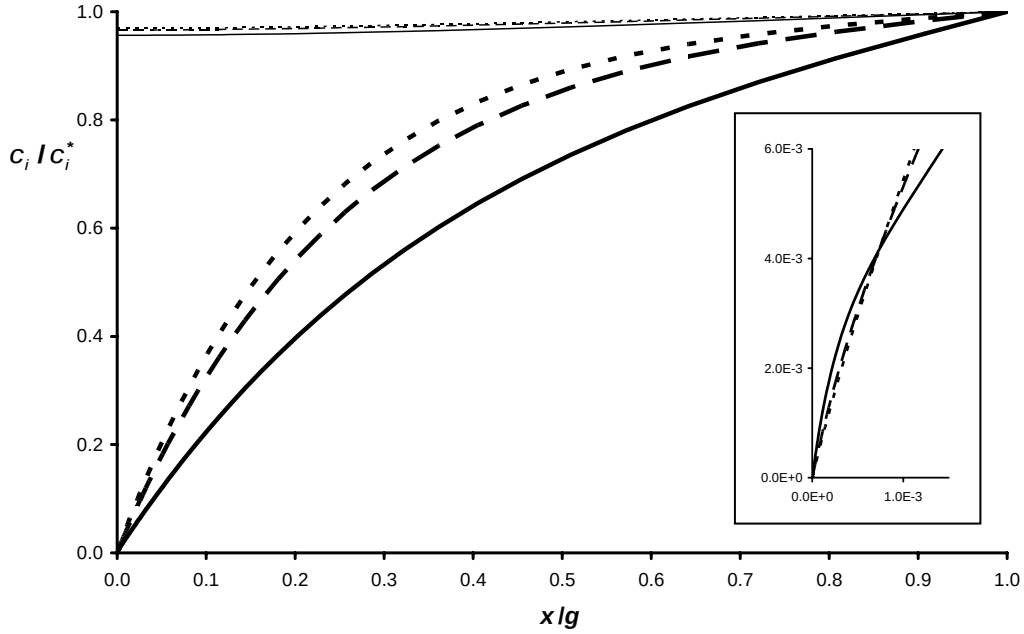

548
549

550 Fig 5: Normalised concentration profiles for the free metal (thick lower lines) and for
551 the CdNTA (thin upper lines). Fixed $c_{T,NTA} = 2\times10^{-3}$ mol m^{-3} and $c_{T,Cd} = 5\times10^{-4}$ mol m^{-3}.
552 Dotted lines stand for $c_{T,Cit} = 0.1$ mol m^{-3}; dashed lines for $c_{T,Cit} = 0.2$ mol m^{-3}; and
553 continuous lines $c_{T,Cit} = 0.8$ mol m^{-3}. The inset shows the crossing of the free metal
554 concentration profiles close to the surface.

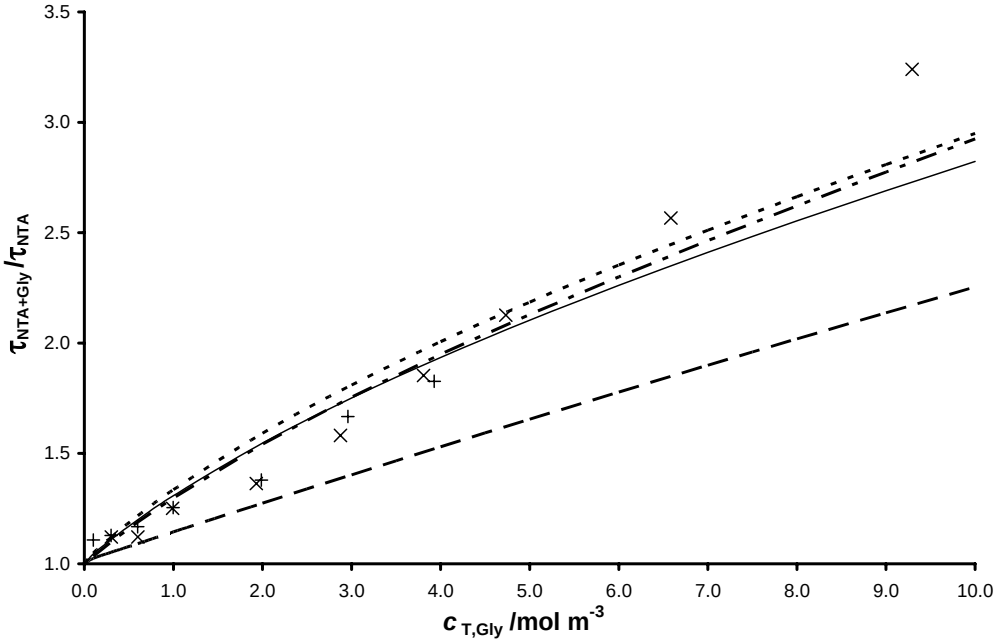

Fig 6: Ratio of fluxes after and before the addition of different amounts of Glycine to a system initially containing $c_{T,NTA} = 2\times10^{-3}$ mol m^{-3} and $c_{T,Cd} = 5\times10^{-4}$ mol m^{-3}. Markers (×) and (+) stand for two replicate series and continuous line for the rigorous solution with parameters in Table 1. Dotted line corresponds to the limiting case of full lability of CdGly (eq (10)) and dashed line stands for the case of non-interacting complexes (eq 4). Dotted-dashed line corresponds to the Zhang and Buffle approximation [15,16].

569

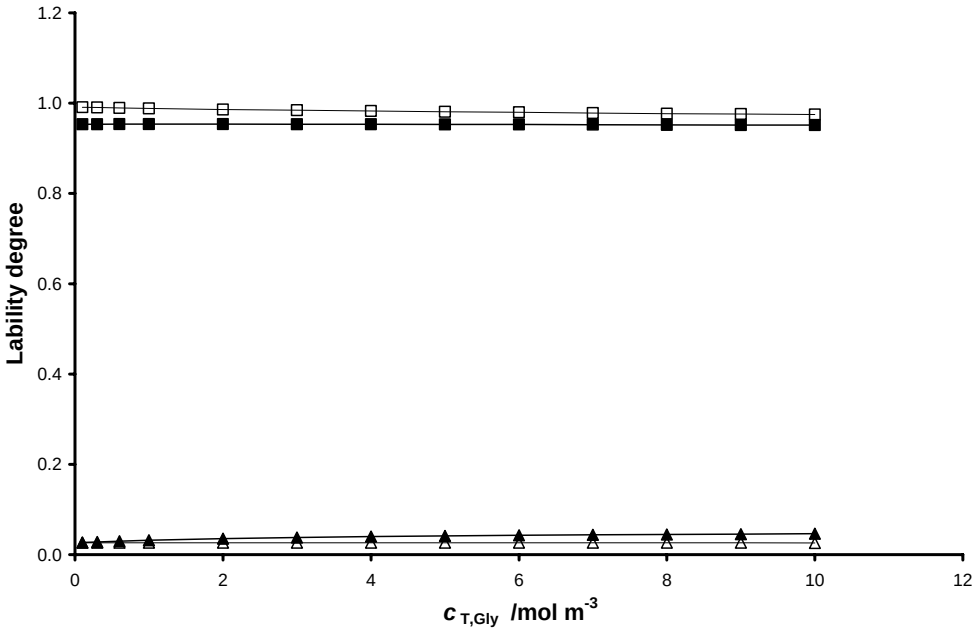

570
571 Fig 7:

572 Lability degrees of complexes Cd+NTA+Glycine along the titration corresponding to
573 Fig 6 with parameters in Table 1. Markers: Full triangle for ${}^{\mathrm{CdNTA}}\xi$; open triangle for the
574 hypothetical case with no interaction ${}^{\mathrm{CdNTA}}\xi^{n=1}$; full square for ${}^{\mathrm{CdGly}}\xi$; open square for
575 the hypothetical case with no interaction ${}^{\mathrm{CdGly}}\xi^{n=1}$.

576

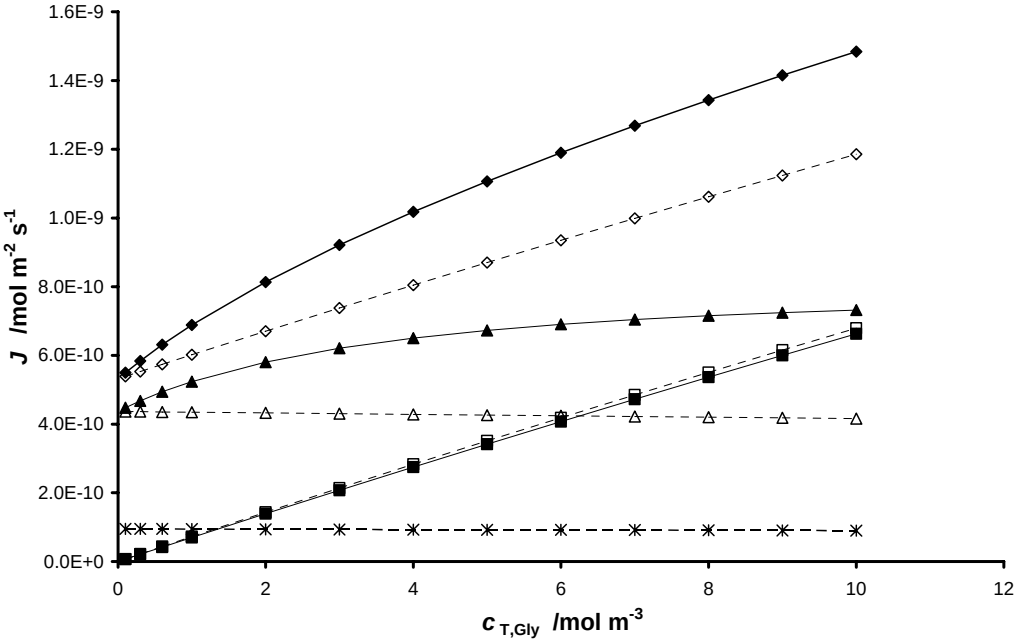

577

578 Fig 8: Fluxes and their components along the titration corresponding to Fig 6 with
579 parameters in Table 1. Lines as in Figure 4. Markers: full diamond for the rigorous total
580 flux, J_M; open diamond for the hypothetical total flux when there is no interaction
581 between complexes $J_M^{n=1}$ (eq 4); asterisk for free metal component, $J_{free} = D_M c_M^* / g$; full
582 triangle for the flux associated to the complex CdNTA, $J_{CdNTA} = D_{CdNTA} c_{CdNTA}^{*\,CdNTA} \xi / g$;
583 full square for the flux $J_{CdGly} = D_{CdGly} c_{CdGly}^{*\,CdGly} \xi / g$; open triangle for the hypothetical flux
584 with no interaction $J_{CdNTA}^{n=1} = D_{CdNTA} c_{CdNTA}^{*\,CdNTA} \xi^{n=1} / g$; and open square for the
585 hypothetical flux with no interaction $J_{CdGly}^{n=1} = D_{CdGly} c_{CdGly}^{*\,CdGly} \xi^{n=1} / g$.

586